7 May 1999

ELSEVIER

Chemical Physics Letters 304 (1999) 336–342

CHEMICAL PHYSICS LETTERS

Reaction dynamics of $Mg(3s4s\,^1S_0)$ with H_2: interference of the MgH product contribution from the lower $Mg(3s3p\,^1P_1)$ state

Dean-Kuo Liu, King-Chuen Lin *

Department of Chemistry, National Taiwan University, and Institute of Atomic and Molecular Sciences, Academia Sinica, Taipei 106, Taiwan, ROC

Received 4 January 1999; in final form 9 March 1999

Abstract

The nascent MgH product distribution obtained in the reaction of $Mg(3s4s\,^1S_0)$ with H_2 was found to be identical to that from the $Mg(3s3p\,^1P_1)$ state. The $4\,^1S_0$ population is found to be much larger by a factor > 18 times than that relaxed to the $3\,^1P_1$ state within the pump–probe delay time. The possibility of a secondary production from the $3\,^1P_1$ state appears to be negligible in the subsequent measurements of the H_2 pressure and the delay time dependences of the MgH rotational lines. These consequences confirm that the MgH product is caused mainly by the direct $Mg(4\,^1S_0)$–H_2 collision, rather than a secondary product from the $3\,^1P_1$ state.

1. Introduction

The nascent rotational distributions of $MgH(v'' = 0 \text{ and } 1, N'')$ in the reaction of $Mg(3s3p\,^1P_1)$ with H_2 have been found to exhibit a bimodal feature, with a major high-N component peaking at large N and a minor low-N component peaking at $N = 7$–8 [1–7]. Such distributions are caused by a reaction mechanism in which Mg approaches H_2 in a side-on attack. The bent-shape collision complex may then proceed via a nonadiabatic transition to the ground state surface. The anisotropic interaction of the ground-state potential energy surface (PES) in the exit channel determines the microscopic branching ratio.

The reaction mechanism of a higher state $Mg(3s4s\,^1S_0)$ with H_2 has also been studied recently [8]. The resulting MgH product distribution was found to be identical to that obtained by the $Mg(3s3p\,^1P_1)$ reaction. To study the reaction dynamics of the high-lying atomic system, one should be very cautious to avoid reaction product contributions from the relaxed lower atomic states that may interfere with the atomic state of interest. Our previous work did not clarify whether the MgH product may be caused by the reaction from the relaxed $3\,^1P_1$ state [8]. The population ratio between the Mg $3\,^1P_1$ and $4\,^1S_0$ state within the pump–probe delay time has not been examined quantitatively. Instead, a rough estimation of population relaxed to $3\,^1P_1$ was made in terms of the spontaneous emission coefficient of

* Corresponding author. Fax: +886 2 2362 1483; e-mail: kclin@hp9k720.iams.sinica.edu.tw

0009-2614/99/$ - see front matter
PII: S0009-2614(99)00332-2

2.6×10^7 s^{-1} for the radiative relaxation from $4\,^1S_0$ to $3\,^1P_1$ [9] [1]. During the delay time adopted, the estimated value suggested that $< 25\%$ of the MgH population contribution may result from reaction of the relaxed $3\,^1P_1$ state. This would be true if the direct chemical reactions with H_2 of $Mg(3s4s\,^1S_0)$ and $(3s3p\,^1P_1)$ occurred at the same rate.

The $4\,^1S_0 \rightarrow 3\,^1P_1$ relaxation may be through the following three channels: collisional deactivation, spontaneous emission, and stimulated emission. Among them, the stimulated emission process could produce $Mg(3s3p\,^1P_1)$ at a rate much faster than the neutral $Mg(3s4s\,^1S_0)$ radiative lifetime or even the pump–probe delay time [11]. Since the spontaneous emission lifetime of $Mg(3s4s\,^1S_0)$ of 39 ns [9] is expected to be larger than the effective lifetime of $Mg(3s3p\,^1P_1)$ at the previous experimental conditions, there is a good possibility that efficient stimulated emission could have been occurring in the previous system if a population inversion between these two states is reached early in the pump laser pulse. The $Mg(3s4s\,^1S_0)$–$Mg(3s3p\,^1P_1)$ transition may proceed alternatively via the collisional deactivation process. According to ab initio calculations [8], there is an adiabatic avoided crossing of the attractive $Mg(3s4s\,^1S_0) \cdot H_2\,[^1A_1]$ potential curve with the very repulsive $Mg(3s3p\,^1P_1) \cdot H_2\,[^1A_1]$ potential curve; this could facilitate the collisional deactivation process, especially if the high-energy Rydberg potential surface does not couple readily with other much lower-energy valence potential surfaces of $Mg(^1P_1) / H_2(^1B_2, {}^1B_1)$. Given the large Mg/H mass disparity, almost all of the 1.1 eV product translational energy gained could go to the lighter H, so that a subsequent reaction of the $Mg(3s3p\,^1P_1)$ produced in the collisional deactivation with another H_2 molecule will be essentially the same as that of a thermal $Mg(3s3p\,^1P_1)$ atom populated by one-photon laser excitation from ground-state $Mg(3s3s\,^1S_0)$. This possibility may be consistent with the experimental observation.

Our previous work does not present convincing experimental evidence that the obtained product distribution is truly nascent and from a direct reaction of $Mg(3s4s\,^1S_0)$ with H_2. From the above arguments, the $MgH(v'', N'')$ observed may be considered to be primarily a result of reaction of $Mg(3s3p\,^1P_1)$ with another H_2 molecule. This speculation is essentially based on the assumption that the population relaxed to the $3\,^1P_1$ state within the pump–probe delay time should be comparable to or even larger than that in the $4\,^1S_0$ state, so that the chemical reaction may be considered to stem from the $3\,^1P_1$ state rather than from the $4\,^1S_0$ state. In this work, we have conducted a series of experiments for comparison of the populations between these two states and examination of the nascent conditions adopted previously. As a supplement to the previous work, the obtained consequences are conducive to clarifying that the $MgH(v'', N'')$ distribution observed is directly initiated by the $Mg(3s4s\,^1S_0)$ state, and the contribution from the secondary reaction of the $Mg(3s3p\,^1P_1)$ state due to relaxation via the above processes is negligible.

2. Experimental set-up

The experimental set-up is similar to the one used in our previous work [8]. Briefly, two dye lasers, each pumped by an individual Nd:YAG laser, were employed as the radiation sources. The pump laser, which was operated at 459.74 nm, was used to prepare the population in the $4\,^1S_0$ state via a two-photon absorption. The unfocused beam was sent through a pinhole of 6 mm diameter, and the output energy was adjusted in the range of 8–9 mJ. The temporal evolutions of the populations either in the $4\,^1S_0$ or in the relaxed $3\,^1P_1$ state were monitored respectively by a probe laser, of which the time delay relative to the pump laser was varied successively. The probe laser was used to excite the atomic $8p\,^1P_1 \rightarrow 3d\,^1D_2$ laser-induced fluorescence (LIF) of the $4\,^1S_0$ population using the $4s\,^1S_0 \rightarrow 8p\,^1P_1$ transition at 628.93 nm with the DCM dye, and to excite the atomic $5d\,^1D_2 \rightarrow 3p\,^1P_1$ LIF of the $3\,^1P_1$ population using the $3p\,^1P_1 \rightarrow 5d\,^1D_2$ transition at 470.3 nm with the coumarin 480 dye. In the former excitation, the emission from $8p\,^1P_1$ to $3d\,^1D_2$ at the wavelength of 769.23 nm was monitored, while in the latter one the emission from $5d\,^1D_2$ either to

[1] The spontaneous emission coefficient of 2.6×10^7 s^{-1} for the $4\,^1S_0 \rightarrow 3\,^1P_1$ transition corresponds to a lifetime of 39 ns. The spontaneous emission coefficient for the $5\,^1D_2 \rightarrow 3\,^1P_1$ transition is 1.6×10^7 s^{-1}, in agreement with that reported by Fischer [10].

$3p\,^1P_1$ at 470.3 nm or to $4s\,^3S_1$ at 661.77 nm was monitored. The energy fluence of the probe laser was adjusted to be large enough to achieve a saturation LIF threshold.

The LIF signal thus obtained was collimated onto a monochromator and detected by a photomultiplier tube, closely attached and enhoused in a cooler at -21°C. The quantum efficiencies of the photomultiplier tube (EMI 9658B) correspond to 4% and 21%, respectively, for the detection wavelengths at 769.23 and 470.3 nm. The grating of the monochromator is blazed at 600 nm. The transmissions for the wavelengths at 769.23 and 470.3 nm are roughly the same, when the slit width is open to 0.15 mm used in this work. For monitoring the IR stimulated emission of the $4\,^1S_0 \rightarrow 3\,^1P_1$ transition, the probe laser was fired first in this work, and then the time delay was varied to cross the pump laser pulse. The related partial energy level diagram related is depicted in Fig. 1.

For examination of the nascent state of the MgH product obtained, specific low and high rotational lines were selected, respectively, and studied as a function of delay time and H_2 pressure. The pump–probe method was similarly employed, but the pump laser was fired ~ 10 ns before the probe laser. The line intensity was represented by its area. Like the previous work [8], the Mg metal in a five-armed cross heat-pipe oven was heated to 750–760 K, corresponding to a Mg vapor pressure of 40–50 mTorr.

3. Results and discussion

Fig. 2 shows the time-resolved atomic LIFs of the $4\,^1S_0$ state using the $4s\,^1S_0 \rightarrow 8p\,^1P$ excitation and the $3\,^1P_1$ state using the $3p\,^1P \rightarrow 5d\,^1D$ excitation. To obtain such results for population evolution, the probe laser was fired either before or after the pump pulse. The pump–probe delay time was varied successively. The zero delay time is defined as that when the falling edge of the probe laser pulse begins to overlap the rising edge of the pump laser pulse. The saturation of the LIF can be achieved by increasing the probe laser energy. In the figure, for atomic

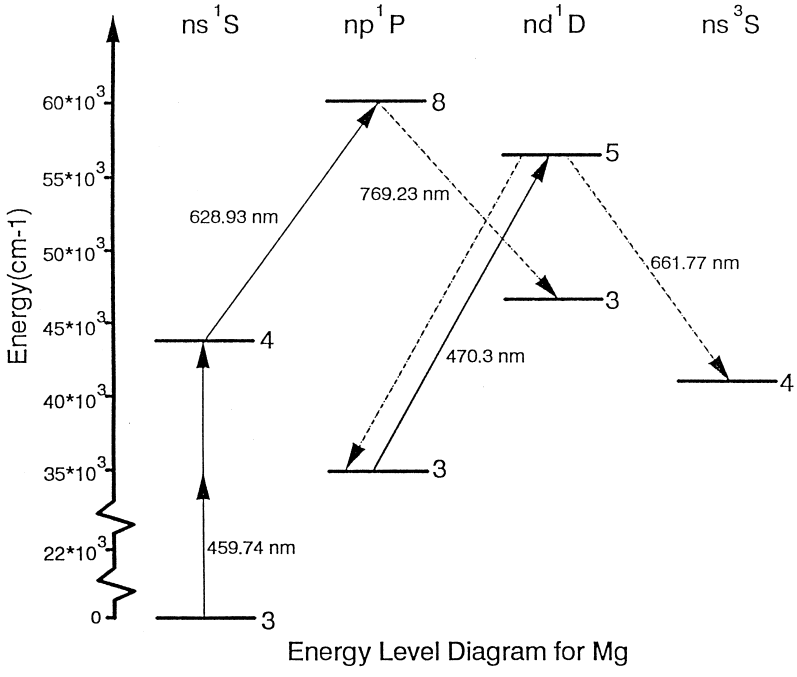

Fig. 1. Energy level diagram of Mg. The solid lines denote the excitation processes conducted by either the pump or the probe laser, while the dashed lines are the emission processes detected.

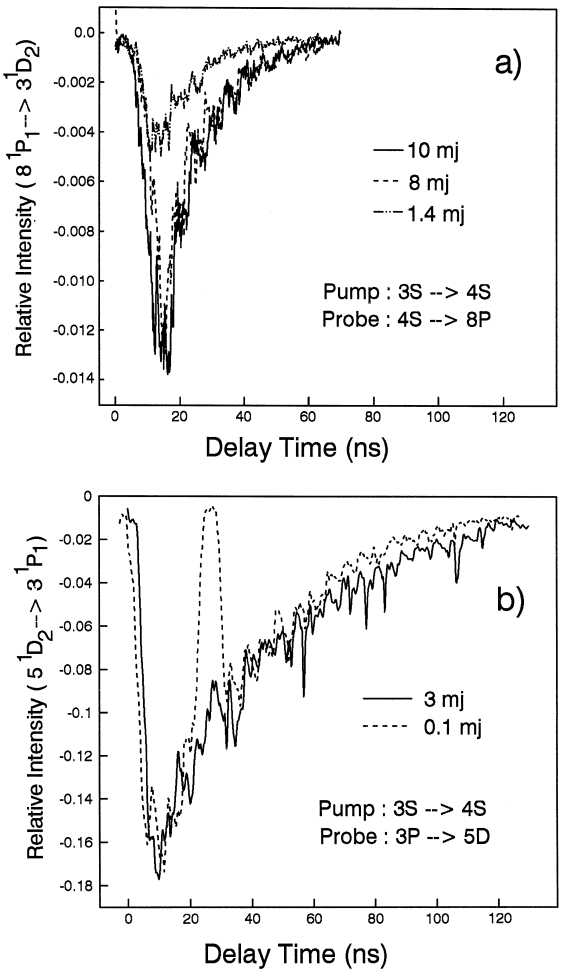

Fig. 2. Temporal evolution of the fluorescence intensity related to the population in the Mg($4\,^1S_0$) and Mg($3\,^1P_1$) states. The initial population is prepared in the $4\,^1S_0$ state by two-photon excitation, while the probe laser is used to excite atomic laser-induced fluorescence (LIF) proportional to the $4\,^1S_0$ and $3\,^1P_1$ state populations, respectively. The schemes for the excitation and emission processes for these two cases are referred to in the text. The probe laser is fired either before or after the pump pulse. The delay time (pump–probe) is varied successively to cross the pump laser pulse. The saturation of the LIF is achieved with an increase of the probe laser energy. (a) The excitation process is saturated with the probe laser energy of 8–10 mJ, in comparison with the unsaturated LIF signal at 1.4 mJ. (b) The saturation is reached with the probe laser energy up to 3 mJ, but the profile of the stimulated emission becomes broadened to merge with the spontaneous emission profile.

LIF of the $4\,^1S_0$ state, the excitation process is saturated as the probe laser energy is increased from 1.4 to 8 mJ. In contrast, for the atomic LIF of the $3\,^1P_1$ state, the saturation condition is met as the probe laser energy is increased to 3 mJ. Such optical saturation offers an advantage for evaluating the state population of interest. The fraction of population promoted from the initial to the excited state may be simplified to the ratio of their state degeneracies. Therefore, for evaluation of the state population one needs to consider only the related spontaneous emission coefficient (A_{fi}). To our knowledge, unfortunately the spontaneous emission coefficient for the $8p\,^1P_1 \rightarrow 3d\,^1D_2$ transition is not available in the literature. The *gf* values (g: state degeneracy; f: oscillator strength) for the $3d\,^1D_2 \rightarrow 7p\,^1P_1$ and $3p\,^1P_1 \rightarrow 5d\,^1D_2$ transitions are found to be 0.0086 and 0.424, respectively [10]. The spontaneous emission coefficients correspond to 3.23×10^5 and 2.55×10^7 s^{-1}, respectively [9,12]. Since the transition probability decreases markedly with increasing the difference of the principal quantum number [13], the A_{fi} value for the $8p\,^1P_1 \rightarrow 3d\,^1D_2$ transition is anticipated to be smaller than the value of 3.23×10^5 s^{-1} for the $7p\,^1P_1 \rightarrow 3d\,^1D_2$ transition.

The population ratio of $4\,^1S_0 / 3\,^1P_1$ may be evaluated by

$$\frac{N_{4S}}{N_{3P}} = \frac{S_{4S}/G_{4S}D_{4S}A_{4S}}{S_{3P}/G_{3P}D_{3P}A_{3P}}, \qquad (1)$$

where S is the intensities for the time-resolved atomic LIFs of the $4\,^1S_0$ and $3\,^1P_1$ states. The ratio of S_{4S} to S_{3P} was estimated to be $1/20$ from the integrated temporal profiles within the delay time of ~ 25 ns (Fig. 2), which was equivalent to 10 ns adopted in the previous experimental set-up. G denotes the ratio of level degeneracies, i.e., $G_{4S} = g_{8P}/(g_{4S} + g_{8P}) = 3/4$ and $G_{3P} = g_{5D}/(g_{3P} + g_{5D}) = 5/8$. D is the quantum efficiency of the photomultiplier tube at the detection wavelength. As reported previously, the D values are 4% and 21%, respectively, at 769.23 and 470.3 nm. A is the spontaneous emission coefficient. Since the A value for the $8p\,^1P_1 \rightarrow 3d\,^1D_2$ is unknown, we adopted $A(7p\,^1P_1 \rightarrow 3d\,^1D_2) = 3.23 \times 10^5$ s^{-1} and $A(5d\,^1D_2 \rightarrow 3p\,^1P_1) = 2.55 \times 10^7$ s^{-1}. Substituting the above values in Eq. (1), accordingly, we have obtained a population ratio of $4\,^1S_0 / 3\,^1P_1$ to be 18 within the delay time of ~ 25 ns (Fig. 2).

Since the A value for the $8p\,^1P_1 \rightarrow 3d\,^1D_2$ transition should be smaller than that for the $7p\,^1P_1 \rightarrow 3d\,^1D_2$ transition [13], the $4\,^1S_0 / 3\,^1P_1$ population ratio is actually larger than 18, if the A_{fi} $(8p\,^1P_1 \rightarrow 3d\,^1D_2)$ value may have been considered.

If the population in the $3\,^1P_1$ state, accumulated through various relaxation processes within the pump–probe delay time, is large enough, the subsequent collision with another H_2 molecule may well result in the MgH product with a good signal-to-noise ratio. We may think about this possibility. The initial population in the $4\,^1S_0$ state prepared by two-photon excitation is ordinarily less than that in the $3\,^1P_1$ state excited directly through a one-photon process. This is due to the fact that the excitation cross-section for the two-photon process is much less than that for the one-photon process unless the laser energy applied is enhanced substantially. According to our observation, the signal intensities for the MgH band-head obtained via either one- or two-photon processes are comparable, when the energies of the unfocused pump laser are adjusted to be 8–11 and 0.1 mJ, respectively, for direct excitation of the $4\,^1S_0$ and $3\,^1P_1$ state, while the other experimental conditions remained the same. Recently, we have further conducted the measurement of MgH$(v = 0, N)$ intensities obtained by initial excitation either to the $4\,^1S_0$ or to the $3\,^1P_1$ state. The excitation processes are optically saturated, so that the excited populations may be evaluated in terms of the related state degeneracies. The MgH$(v = 0, N)$ intensity initiated by the $4\,^1S_0$ state is found to be ~ 1.5 times larger than that by the $3\,^1P_1$ state [14]. Accordingly, while considering the $4\,^1S_0 / 3\,^1P_1$ population ratio evaluated above, one may not anticipate a product distribution with a reasonable signal-to-noise ratio obtained by the secondary reaction of the $3\,^1P_1$ atoms relaxed from the $4\,^1S_0$ state.

As shown in Fig. 2b, a rapid decay of the emission in the $5d\,^1D_2 \rightarrow 3p\,^1P_1$ transition is observed, indicating that an IR stimulated emission from $4\,^1S_0$ to $3\,^1P_1$ does occur with a response time as fast as the pump laser [11]. The stimulated emission decays dramatically to zero within 30 ns. Then an ordinary

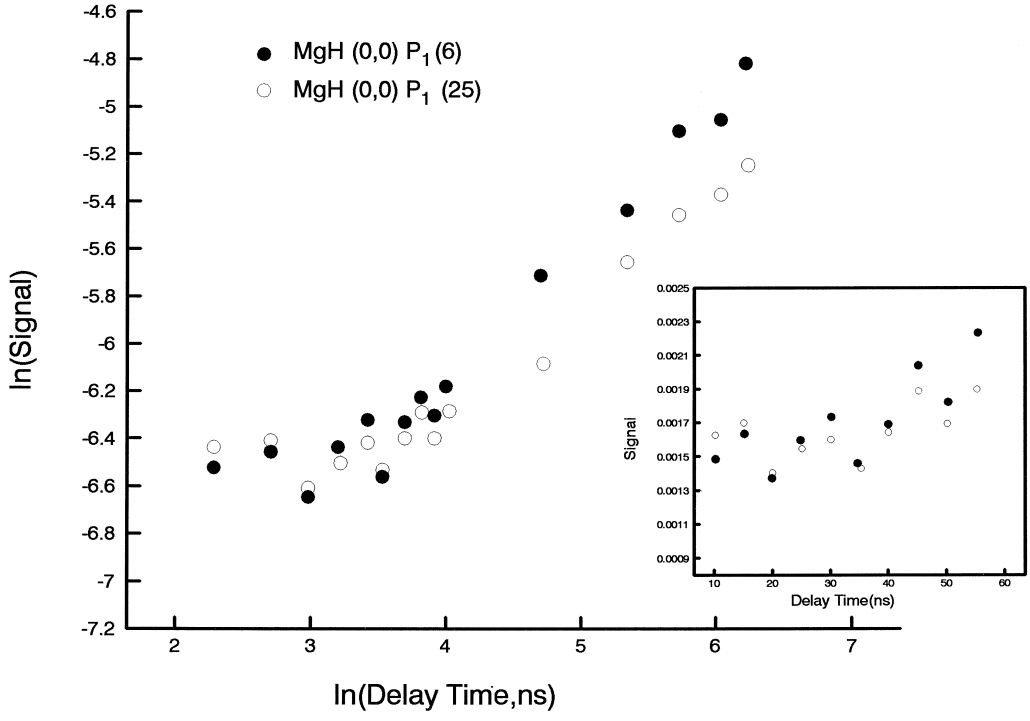

Fig. 3. The LIF signals of MgH$(0, 0)$ $P_1(6)$ and $P_1(25)$ as a function of time delay of the probe laser relative to the pump laser at the H_2 pressure of 3 Torr. The signals are on a scale normalized to $I(\mathrm{P1}(6)) = I(\mathrm{P}_1(25)) = \mathrm{e}^{-6.5}$.

spontaneous emission profile follows. The profile of fast stimulated emission is broadened to merge with the profile of spontaneous emission, as the probe laser energy is increased. However, the peak intensity remains invariant once the laser energy reaches the threshold of optical saturation (Fig. 2). When the alternative $5d\,^1D_2 \rightarrow 4s\,^3S_1$ emission is monitored, a population evolution similar to Fig. 2b is obtained. As reported elsewhere [15,16], the IR stimulated emission tends to be enhanced in a wave-mixing process usually at an atomic vapor pressure of several Torr. In Fig. 2b the peak intensity related to the IR stimulated emission is comparable to that of the spontaneous emission. Here we have taken into account the contributions of both types of emissions in the evaluation of $3\,^1P_1$-state population, as described above.

As shown in Figs. 3 and 4, we have measured the intensity of the MgH rotational lines as a function of delay time and H_2 pressure. Note that in these experiments the pump laser is fired before the probe laser. The definition of delay time is thus identical to that adopted in the previous work [8], i.e., the delay time is counted from the falling edge of the pump laser pulse up to the onset of the probe laser pulse. The time delay is varied within the range of 10–400 ns. As shown in Fig. 3, the peak intensities of the MgH(0, 0) $P_1(6)$ and $P_1(25)$ lines appear to weakly depend on the delay time from 10 to 40 ns at a H_2 pressure of 3 Torr. When the delay time is set at 10 ns, on the other hand, a linear proportionality for the H_2 pressure dependence is found within the range of 1.2–7.0 Torr (Fig. 4). The conditions adopted for our previous work [8] lie in this linear pressure region. Therefore, the possibility of production of MgH obtained previously from a secondary collision has been minimized.

Why are the bimodal features of the MgH distributions obtained from $Mg(4\,^1S_0)$ similar to those obtained from $Mg(3\,^1P_1)$? This fact may be rationalized if the energy disposal of 1.1 eV in the ion-pair $Mg^+H_2^-$ complex may be substantially carried away by the H atom. This is possible since the strong instability of H_2^- tends to cause most of the available energy to be partitioned into translation. Similar examples are also found in the $K^* + H_2$ [17,18] and $Cs^* + H_2$ reactions [19–21], which have been demonstrated to follow the harpoon-type mechanism.

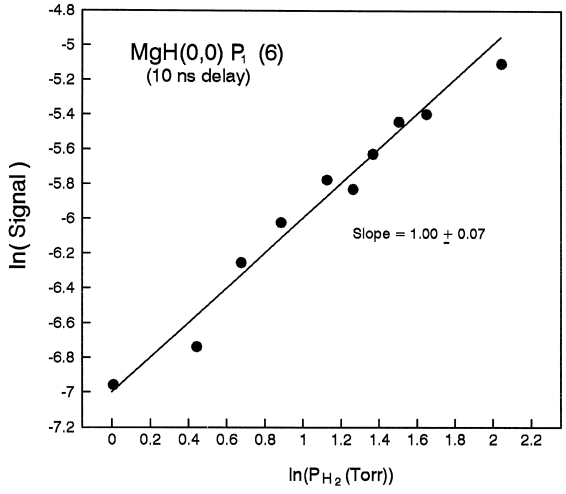

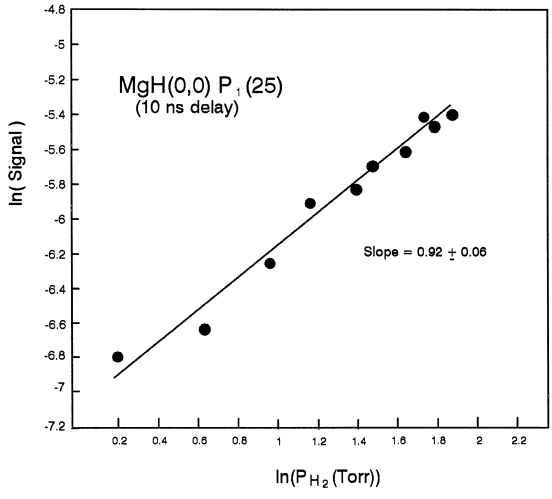

Fig. 4. The H_2 pressure dependence of the LIF signals of MgH(0, 0) $P_1(6)$ and $P_1(25)$ at a time delay of 10 ns.

In these two systems, ~70% and ~90% of the available energies are released as translation, respectively [18,21]. Polanyi and co-workers have developed the related theoretical models characterizing the product energy distribution in the reaction of a three-atom system via a harpoon mechanism [22,23].

In summary, we have conducted a series of experiments to inspect the possibility of a MgH(v'', N'') product contribution from a secondary reaction of the $Mg(3\,^1P_1)$ atoms formed by relaxed atom of the $4\,^1S_0$ atomic state. However, we find that the ob-

tained nascent products are mainly caused by the direct $Mg(4\,^1S_0)$–H_2 reaction.

Acknowledgements

This work is supported by the National Science Council of the Republic of China under contract No. 88-2113-M-002-011.

References

[1] W.H. Breckenridge, H. Umemoto, J. Chem. Phys. 80 (1984) 4168.
[2] W.H. Breckenridge, J.H. Wang, Chem. Phys. Lett. 82 (1985) 4945.
[3] P.D. Kleiber, A.M. Lyyra, K.M. Sando, V. Zafiropulos, W.C. Stwalley, J. Chem. Phys. 85 (1986) 5493.
[4] P.D. Kleiber, A.M. Lyyra, K.M. Sando, S.P. Heneghan, W.C. Stwalley, Phys. Rev. Lett. 54 (1985) 2003.
[5] P. Chaquin, A. Sevin, H. Yu, J. Phys. Chem. 89 (1985) 2813.
[6] K.C. Lin, C.T. Huang, J. Chem. Phys. 91 (1989) 5387.
[7] Y.R. Ou, D.K. Liu, K.C. Lin, J. Chem. Phys. 108 (1998) 1475.
[8] D.K. Liu, K.C. Lin, Chem. Phys. Lett. 274 (1997) 37.
[9] W.L. Wiese, M.W. Smith, B.M. Miles, Atomic Transition Probabilities, vol. II, NSRDS-NBS 22, US Gov. Print. Off., Springfield, VA, 1969.
[10] C.F. Fischer, Can.J. Phys. 53 (1975) 184.
[11] P.D. Kleiber, A.M. Lyyra, S.P. Heneghan, W.C. Stwalley, J. Opt. Soc. Am. B 2 (1985) 522.
[12] J.I. Steinfeld, Molecules and Radiation, MIT Press, Cambridge, MA, 1981, p. 28.
[13] C. Fabre, S. Haroche, in: R.F. Stebbing, F.B. Dunning (Eds.), Rydberg States of Atoms and Molecules, Cambridge University Press, London, 1983, p. 117.
[14] D.K. Liu, K.C. Lin, unpublished results.
[15] P.L. Zhang, Y.C. Wang, A.L. Schawlow, J. Opt. Soc. Am. B 1 (1984) 9.
[16] B.K. Clark, M. Masters, J. Huennekens, Appl. Phys. B 47 (1988) 159.
[17] D.K. Liu, K.C. Lin, J. Chem. Phys. 105 (1996) 9121.
[18] D.K. Liu, K.C. Lin, J. Chem. Phys. 107 (1997) 4244.
[19] A.G. Urena, R. Vetter, Int. Rev. Phys. Chem. 15 (1996) 375.
[20] A.G. Urena, R. Vetter, J. Chem. Soc., Faraday Trans. 91 (1995) 389.
[21] X. Huang, J. Zhao, G. Xing, X. Wang, R. Bersohn, J. Chem. Phys. 104 (1996) 1338.
[22] P.J. Kuntz, E.M. Nemeth, J.C. Polanyi, J. Chem. Phys. 50 (1969) 4607.
[23] P.J. Kuntz, M.H. Mok, J.C. Polanyi, J. Chem. Phys. 50 (1969) 4623.